Available online at http://www.journalcra.com

International Journal of Current Research
Vol. 8, Issue, 01, pp.25250-25259, January, 2016

INTERNATIONAL JOURNAL OF CURRENT RESEARCH

ISSN: 0975-833X

RESEARCH ARTICLE

SYNTHESIS, STRUCTURAL, SPECTRAL AND BIOLOGICAL ANALYSIS OF A CHARGE TRANSFER COMPLEX CRYSTAL OF N, N DIMETHYL 4 AMINO PYRIDINIUM 4 AMINO BENZOATE DIHYDRATE

[1]Mohanbabu, B., [*,2]Bharathikannan, R. and [2]Siva, G.

[1]Department of Physics, Sri Shakthi Institute of Engineering and Technology, Coimbatore- 62, Tamil Nadu, India
[2]Department of Physics, Sri Ramakrishna Mission Vidyalaya College of Arts and Science, Coimbatore - 20, Tamil Nadu, India

ARTICLE INFO

Article History:
Received 05th October, 2015
Received in revised form
10th November, 2015
Accepted 09th December, 2015
Published online 31st January, 2016

Key words:

Antibacterial,
Antifungal,
Antioxidant,
DFT,
SXRD.

ABSTRACT

The charge-transfer complex crystal of N, N dimethyl 4 amino pyridinium 4 amino benzoate dehydrate is synthesised and the complex has been confirmed by studying the spectroscopic results. The crystal structure was comprehended by single crystal X-ray diffraction analysis. The cation and anion are linked through strong hydrogen bond in the molecule. The Mulliken atomic charge and the values of electronegativity and chemical hardness index were calculated for interpreting and predicting the reactive behaviour. The lowering in the HOMO and LUMO energy gap explains the eventual charge transfer interactions that take place within the molecules. Fourier transform infrared (FT-IR) spectroscopic studies were also performed for the identification of different modes present in the compound. This dielectric study highlights the dielectric constant decreases with increase in frequency. The charge transfer crystal was subjected for its biological activity, such as antibacterial, antifungal and antioxidant activity. The antibacterial and antifungal activities of the synthesized complex were examined against various bacteria and fungi species, which exhibited a good antibacterial and antifungal activity compared with standard antibacterial and fungal species. The compound has significant antioxidant activity against free DPPH radicals.

Citation: **Mohanbabu, B., Bharathikannan, R. and Siva, G. P. 2016.** "Synthesis, structural, spectral and biological analysis of a charge transfer complex crystal of n, n dimethyl 4 amino pyridinium 4 amino benzoate dihydrate", *International Journal of Current Research*, 8, (01), 25250-25259.

INTRODUCTION

Over the past few decades, the widespread researches have been carried out on the growth of defect free single crystals as it plays a vibrant role in the areas of optoelectronics, solid state lasers, remote sensing and medical diagnostics (Ogorodnikov *et al*., 2013; Misoguti *et al*., 1996). The Charge transfer (CT) complexes have become an important keystone in the field of biology. The Charge Transfer complex plays an effective role in DNA-binding, antibacterial, antifungal, insecticides and the field of drug receptor binding mechanism (Gutmann *et al*., 1997; Yasutake *et al*., 2003; Palacios *et al*., 2005; Bock *et al*., 2006). The π acceptor charge transfer reactions have been employed positively in pharmaceutical investigation. Therefore CT complexes encouraged widespread research on these kind of complexes (Amin *et al*., 1995; Zhao *et al*., 1999). Moreover, the field of non-linear optical materials and electrical conductivities finds the application of such complexes. For these extensive applications, more works on charge-transfer complexes of acceptors have been carried out. The charge transfer complexes of organic materials are considered for the reason that the special type of interaction is accompanied by transfer of an electron from the donor to the acceptor. Similarly, the protonation of the donor from the acidic acceptors are basis for the construction of ion pair materials.

Pyridine derivatives are prominent materials in the field of biology as they show a wide range of biological properties like antitumor, antibiotics, psychotropic, anti-inflammatory, and antihistaminic activities. This pyridine moiety presences in many large complexes repeatedly with fascinating applications in catalytic, photophysical, and electrochemical field (Goel and Ram, 2009; Al-Hashimy *et al*., 2010). Hence, they have been expected as useful drugs for the treatment of many diseases like myocardial infarction and diarrhea. This has led to the development of new drugs based on pyridine. Because of the above mentioned properties and applications, we study the crystalline perfection and other physical properties of the pyridine based materials. In the presence of nitrogen atom in pyridine ring, the chemical is used as an efficient material for the establishment of charge transfer molecule.

Corresponding author: Bharathikannan, R.
Department of Physics, Sri Ramakrishna Mission Vidyalaya College of Arts and Science, Coimbatore - 20, Tamil Nadu, India.

In this research work, the single crystals of N, N dimethyl 4-amino pyridinium 4-amino benzoate dehydrate (DMAPAB) were grown by slow evaporation solution growth technique in room temperature. The grown crystals were subjected for the various characterization such as single X-ray diffraction analysis, UV–vis spectroscopy, FTIR, and dielectric study. And also, the quantum chemical density functional calculations including Mulliken atomic charges, frontier molecular orbitals, thermal properties and hyperpolarizability have been calculated for the DMAPAB crystals. Furthermore, the synthesised compound is subjected to the biological activities.

Experimental Details

Synthesis and growth of DMAPAB

Single crystal of DMAPAB (C14 H21 N3 O4) was grown by slow evaporation solution growth method at room temperature. One mole of N, N dimethyl 4-amino pyridine and one mole of 4-amino benzoic acid were added and mixed in methanol solvent to obtain the salt of title compound. The solution was mixed and stirred well for about 3 hours to get homogeneous solution using mechanical stirrer. The resulting solution was filtered to remove the suspended impurities. The beaker was covered by ordinary filter paper. Care was taken to minimize the temperature gradient and mechanical shake. The filtrate was kept aside in dust free environment for crystallization process. The crystals of DMAPAB were harvested by slow evaporation technique at the ambient temperature.

Characterisation

The X-Ray diffraction intensities were measured on a Bruker Smart X2S diffractometer at 295K. The well-collimated Mo Kα radiation (λ = 0.71073 Å) and the ω-scan mode were employed. The UV-visible absorption and transmittance spectra were recorded on SYSTRONICS DOUBLE BEAM UV-Vis spectrophotometer operating between 250 and 700 nm. The FT-IR spectrometer using KBr pellets. Dielectric studies were carried out using HIOKI multifrequency LCR meter.

Computational details

Quantum chemical calculations of the title compound were carried out with Gaussian03 software program (Frisch *et al*., 2004) and the GaussView molecular visualization program (Frisch *et al*., 2004). Mulliken atomic charges, Frontier Molecular Orbitals and Thermodynamic Properties values were calculated for the DMAPAB crystal by using B3LYP (Becke's three-parameter hybrid model using the Lee-Yang Parr correlation functional) methods which consist of the Lee–Yang–Parr correlation functional in conjunction with a hybrid exchange functional first proposed by Becke (Becke, 1993; Lee *et al*., 1988). The Donor and the acceptor occupancy and of the stabilization energy of the different overlapping for the title compound was studied by using B3LYP/6-311++G basis set. Furthermore, the dipole moment (μ), the polarizability (α) and the first-order hyperpolarizability (β) of the title compound under study were calculated by B3LYP/6-311++G level.

Antibacterial activity

The antibacterial activity of newly synthesized title compound was tested against Staphylococcus aureus, Bacillus substilis, Klebsiella pneumonia, and Pseudomonas aeruginosa by Kirby–Bauer method (Bauer *et al*., 1996). Media with DMSO solvent was set up as control. The discs measuring 5 mm in diameter were prepared from Whatman No. 1 filter paper sterilized by dry heat at 140^{o} C for 1 h. The sterile discs previously soaked in a concentration of the test compounds were placed in a nutrient agar medium. The petri plates were invested and kept in an incubator for the time period of 24 h at the temperature of 37^{o} C and growth was monitored visually. The screening was performed at 100 lg/mL concentration of test complexes and antibiotic disc. Ciprofloxacin (10μg/disc) was used as control. Logarithmic serially two fold diluted amount of test complexes and controls was inoculated within the range 104–105 cfu/mL. To obtain the diameter of zone, 0.1 ml volume was taken each and spread on agar plates. The number of colony forming units (cfu) was counted after 24 h of incubation at 35o C. After incubation the zone of inhibition was measured and expressed as mm in diameter (Collins, 1976; Cruickshank *et al*., 1995).

Antifungal activity

The newly synthesized compound was also screened for its antifungal property against Aspergillusniger, Aspergillusflavus, Aspergillusfumigatus and Penicillium sp. in DMSO solvent by using standard agar disc diffusion method. The synthesized compound was dissolved in DMSO as a solvent and media with DMSO was set up as a control. All cultures were routinely maintained on Sabouraud Dextrose Agar (SDA) and incubated at 28 °C. Spore formation of filamentous fungi was formed from seven days old culture on sterile normal solution, which was diluted to approximately 105 cfu/mL and the culture was centrifuged at 1000 rpm. The pellets were resuspended and diluted in sterile Normal Saline Solution (NSS) to obtain a viable count 105 cfu/mL. With the help of spreader, 0.1 mL of approximately diluted fungal culture suspension was spreaded on agar plates. The fungal activity of compound was compared with Clotrimazole (10 μg /disc) which is used as a standard drug. The cultures were incubated for 48 h at 37 ºC and the growth was monitored. Antifungal activity was determined by measuring the diameters of the zone (mm) in triplicate sets.

Antioxidant activity

DPPH radical scavenging activity of extract was determine according to the method reported by Blois (1958). An aliquot of 0.5 ml of sample solution in methanol was mixed with 2.5 ml of 0.5 mMmethanolic solution of DPPH. The mixture was shaken vigorously and incubated for 30 min in the dark at room temperature. The absorbance was measured at 517 nm using UV spectrophotometer. Ascorbic acid was used as a positive control. DPPH free radical scavenging ability (%) was calculated by using the formula. % of inhibition = absorbance of control – absorbance of sample / absorbance of control ×100. The ascorbic acid was used as standard molecule for comparison of the tested sample. The principle in this method is that the antioxidant (synthesized compound) reacts with the

stable DPPH free radical (deep violet colour) and convert it to 2, 2-diphenyl-1-picrylhydrazine with decolourisation. The degree of decolourisation shows the scavenging ability of the antioxidant compound.

RESULTS AND DISCUSSION

Single crystal X-ray diffraction analysis

The single crystal X-ray diffraction data is collected with graphite–monochromated Mo Kα radiation (λ = 0.071073 nm) at 293 K. A suitable sample of size 0.22 mm x 0.21 mm x 0.15 mmis chosen and mounted on the goniometer. Cell refinement and data reduction are carried out using CAD-4 EXPRESS (Enraf-Nonius, 1994) and XCAD4 (North *et al*., 1968). The structures are solved by direct methods procedure using SHELXS-97 and refined by full-matrix least-squares on F^2 using SHELXL -97 program (Sheldrick, 1997). All non-hydrogen atoms are anisotropically refined. The hydrogen atom positions are fixed at geometrically calculated distances to allow riding on the parent atoms to which they are attached. The molecular graphics are prepared by using the ORTEP (Farrugia, 1997).

From the analysis it is found that title compound crystallizes in monoclinic system with space group $P2_{(1)}/c$. The lattice parameters obtained are a = 9.3575(6), b = 9.8337(6), c = 10.2294(6), alpha = 65.671°, Beta = 69.971°, gamma = 89.150° and the unit cell volume is 797.02 Å^3. The N, N dimethyl 4 amino pyridine appears in crystalline lattice as single protonated cation and 4-amino benzoate is present as deprotonated anion in the title compound. The X-ray single crystal structure shows the presence of protonated N, N dimethyl 4 aminopyridiniumcation and gives intermolecular hydrogen bonding associations. The ORTEP representation of the compound is shown in Figure 1. Crystal data and structure refinement for DMAPAB are depicted in the Table 1. In N, N dimethyl 4 amino pyridine, the pyridine nitrogen is more basic when compared to the dimethyl amino group. This lower basicity of $N(CH3)_2$ is due to the resonance interaction between $N(CH3)_2$ and the pyridine ring. Hence, the pyridine ring nitrogen can be immediately protonated in preference to the dimethyl amino group. The process of protonation leads to the widening of C1–N6–C5 angle in the pyridine ring to 118.56°, compared to 115° in neutral N, N dimethyl 4 amino pyridine. Weaker cross-links between the chains are formed by N-H ….O bonds.

Table 1. Crystal data and structure refinement for DMAPAB

Identification code	shelxl
Empirical formula	C14 H21 N3 O4
Formula weight	295.34
Temperature	293(2) K
Wavelength	0.71073 Å
Crystal system, space group	TRICLINIC, P-1
Unit cell dimensions	a = 9.3575(6)A alpha = 65.671(4)deg. b = 9.8337(6)A beta = 69.971(3)deg. c = 10.2294(6)A gamma = 89.150(4)deg.
Volume	797.02(8)A^3
Z, Calculated density	2, 1.231Mg/m^3
Absorption coefficient	0.091mm^-1
F(000)	316
Crystal size	0.22 x 0.21 x 0.15 mm^3
Theta range for data collection	2.3 to 26.48 deg.
Limiting indices	-11<=h<=11, -11<=k<=12, -12<=l<=12
Reflections collected / unique	11932 / 3292 [R(int) = 0.0266]
Completeness to theta	26.48 99.9 %
Absorption correction	Semi-empirical from equivalents
Max. and min. transmission	0.991 and 0.984
Refinement method	Full-matrix least-squares on F^2
Data / restraints / parameters	3292 / 0 / 209
Goodness-of-fit on F^2	1.055
Final R indices [I>2sigma(I)]	R1 = 0.0508, wR2 = 0.1468
R indices (all data)	R1 = 0.0918, wR2 = 0.1767
Largest diff. peak and hole	0.220 and -0.243 e.A^-3

Table 2. Molecular Property of the DMAPAB crystal

Property	Values
Ionisation energy (I)	0.18414 eV
Electron affinity (A)	0.07507 eV
Electronegativity(χ)	0.129605 eV
Chemical Potential (μ)	- 0.129605 eV
Chemical Hardness (η)	0.054535 eV
Softness (S)	9.168424 eV^{-1}
Global Electrophilicity Index (ω)	0.154006 eV

Table 3. Thermodynamical parameter

Self-consistent field Energy (a.u.)		-1010.6059
Zero point energy (Kcal/Mol)		225.80347
Rotational constant(GHZ)		0.79108
Rotational temperature (Kelvin)		0.03797
Energy(E)	Translational	0.889
(KCal/Mol)	Rotational	0.889
	Vibrational	234.666
	Total	236.443
Specific heat (C_v)	Translational	2.981
(Cal/	Rotational	2.981
Mol-Kelvin)	Vibrational	55.326
	Total	61.287
Entropy(S)	Translational	42.944
(Cal/	Rotational	35.120
Mol-Kelvin)	Vibrational	59.909
	Total	137.973
Dipole moment (Debye)		15.0674

Table 4. Antibacterial activity of DMAPAB Complex

S.No.	Organisms	Ciprofloxacin	Dmapab
1.	Staphylococcus aureus	33	32
2.	Bacillus substilis	28	21
3.	Klebsiellapneumoniae	27	22
4.	Pseudomonas aeruginosa	32	29

Table 5. Antifungal activity of DMAPAB Complex

S.No.	Organisms	Clotrimazole	Dmapab
1	*Candida albicans*	16	24
2	*Aspergillusniger*	25	21
3	*Aspergillusfumigatus*	23	25

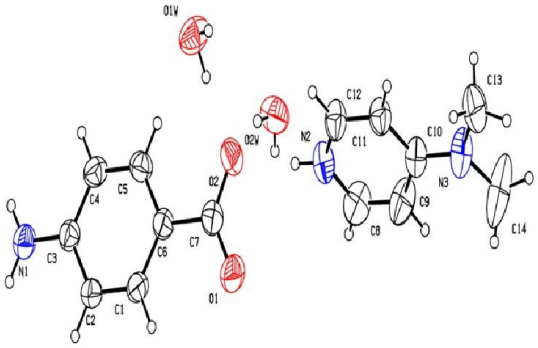

Fig. 1. The ORTEP diagram of DMAPAB crystal

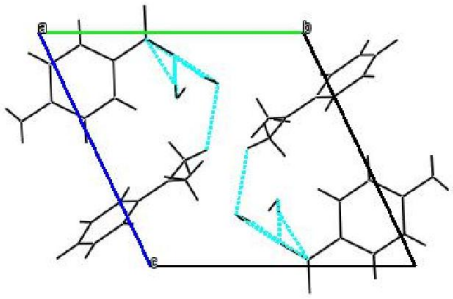

Fig. 2. The packing diagram of DMAPAB crystal

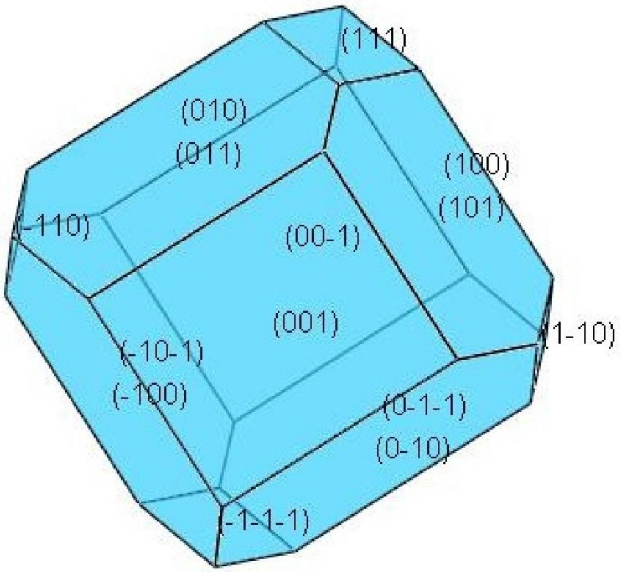

Fig. 3. The morphology of DMAPAB crystal

The C-H ….O hydrogen bonding is responsible for the tight packing of molecules in the unit cell leading to a three dimensional network. The crystal packing diagram of the compound along the b axis is shown in Figure 2. The morphology of the grown crystal is obtained from the Mercury program (Macrae *et al*., 2008) and is shown in the Figure 3.

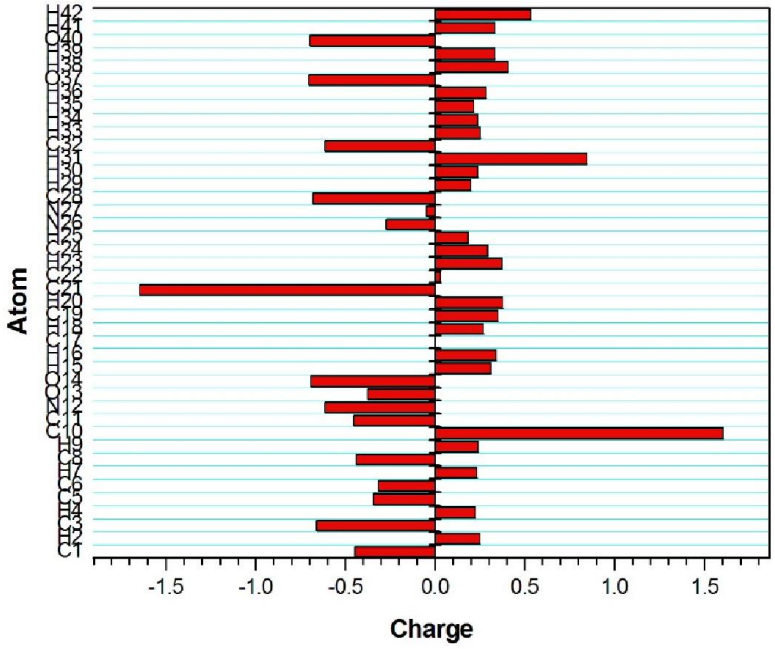

Fig. 4. The Mulliken atomic charges of DMAPAB crystal

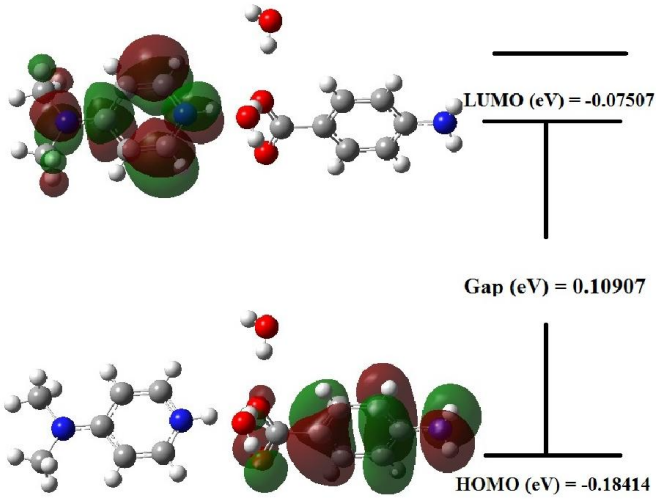

Fig. 5. The distributions and energy levels of HOMO and LUMO orbitals for DMAPAB crystal

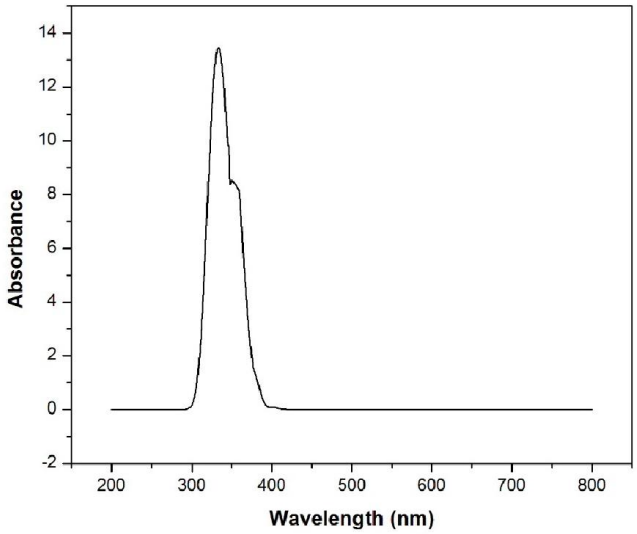

Fig. 6. The UV absorption spectrum of the DMAPAB crystal

Mulliken atomic charge distribution

The calculation of atomic charges has a vital role in the application of quantum chemical calculation to molecular system. This charge distribution on molecules has significant influence in many properties such as dipole moment, electronic structure, polarizability. Also, the mulliken net charges of title compound is calculated and shown in Figure 4. From the figure, it can be observed that the atomic charges of DMAPAB are ranging from -1.64 and +1.60. Atom C21 which is attached to the dimethyl amine group, which has the highest negative charge about -1.6. The atoms O13 and O14 of carboxylic acid group are also having more negative charge but not more than other C21 atom. Atom C10 has the highest positive charge (1.6) as it has attached to the carboxylic acid group of 4 amino benzoate moiety. The proton H31 has more positive charge than other H atoms in the molecule since the atom H31 is between atom N26 of pyridine ring and O14 of carboxylic group. The results of these analysis reveal that there is proton transfer from 4 amino benzoate to dimethyl 4 amino pyridinium. The variations in atomic charges of hydrogen atoms are formed of the formation of hydrogen bonding. Nevertheless, the sum of Mulliken atomic charges of all atoms of DMAPAB molecule maintains the charge neutrality. Mulliken population method can be helpful to know the reactive behaviour of a chemical systems in both electrophilic and nucleophilic reactions.

Analysis of Frontier Molecular Orbitals

Highest occupied molecular orbital (HOMO) and lowest unoccupied molecular orbital (LUMO) are the most important frontier molecular orbitals (FMOs) which play a vital role in the optical and electric properties, quantum chemistry and UV–vis spectra. The chemical stability of the molecule also depends on the nature of the FMO (Parthasarathi *et al*., 2004). The HOMO represents the ability to donate an electron and LUMO as an electron acceptor represents the ability to accept an electron, whereas dealing with molecular orbitals interaction, the two orbitals (HOMO and LUMO) of the compound. These orbitals are a pair of orbitals in the compound, which allows them to interact more strongly. In order to evaluate the energetic behaviour of the DMAPAB, the energies of HOMO, LUMO and the orbital energy gaps are calculated. The pictorial representation of HOMO and LUMO are shown in the Figure 5. The energy gap between HOMO and LUMO also determines the chemical reactivity and chemical hardness and softness of the molecule (Kosar and Albayrak, 2011). Figure 5 shows the distributions and energy levels of HOMO and LUMO orbitals for DMAPAB in gaseous phase.

Ionisation energy (I) is directly proportional to the electrochemical oxidation potentials of the compounds whereas electron affinity (A) give an idea about the stability of free radicals and anions. These two are of great importance in the determination of biochemical pathways for electron transfer, photosynthesis, oxidative phosphorylation, and oxidative stress. The ionisation energy and electron affinity can be expressed through HOMO and LUMO orbital energies by connecting it with Hartree-Fock SCF theory and invoking Koopmans' theorem (Koopmans, 1993) as:

$$I = -E_{HOMO} \quad \text{.....(1)}$$

$$A = -E_{LUMO} \quad \text{.....(2)}$$

From the value of ionization energy and electron affinity, the electro negativity (χ), chemical potential (μ), chemical hardness (η), softness (S) are also calculated (Chermette, 1999).

$$\chi = 1/2(E_{HOMO} + E_{LUMO}) \quad \text{.....(3)}$$

$$\mu = -\chi = 1/2(E_{HOMO} + E_{LUMO}) \quad \text{.....(4)}$$

$$\eta = (I - A)/2 \quad \text{.....(5)}$$

S= 1/2η)

Parr *et al*. (1999) have proposed the global electrophilicity power of a system and also its property to soak up electrons as

$$\omega = \mu^2 / 2\eta \quad \text{.....(6)}$$

This index measures the stabilisation in energy when the system acquires an additional electronic charge from the environment. By definition, it encompasses both the ability of an electrophile to acquire additional electronic charge and the resistance of the system to exchange electronic charge with the environment. Electrophilicity contains information about both electron transfer (chemical potential) and stability (hardness), it is expected to be a better descriptor of global chemical reactivity. The molecular properties of DMAPAB are given in the Table 2.

UV- visible spectral analysis

To study linear optical characteristics of the material, the UV-Vis-NIR spectral analysis is carried out on the material. Ultra violet and visible radiation interacts with matter which causes electron transitions from the ground to a high energy state. UV absorption spectra arise from the transition of electrons within a molecule from a lower electronic energy level to a higher one. Three distinct types of electrons are involved in organic molecules such as the σ-electrons (involved in saturated bonds), the π-electrons (involved in bonding between the atoms in molecules and in the electrons which can be excited by UV radiation). When an atom or molecule absorbs the energy, electrons are promoted from their ground state to an excited state. The grown crystals of DMAPAB are subjected to UV-Vis-NIR spectral analysis in the wavelength range from 200 to 800 nm. The electronic transition between 'non-bonding' n orbital and anti-bonding π orbital represented as π*, a strong absorption took place around 334 nm. This absorption is shown in Figure 6. The crystal is entirely transparent beyond cut-off wavelength up to 800 nm.

FTIR Analysis

The FTIR spectrum of DMAPAB was recorded using BRUKER IFS 66V model spectrophotometer, which is shown in Figure 7.

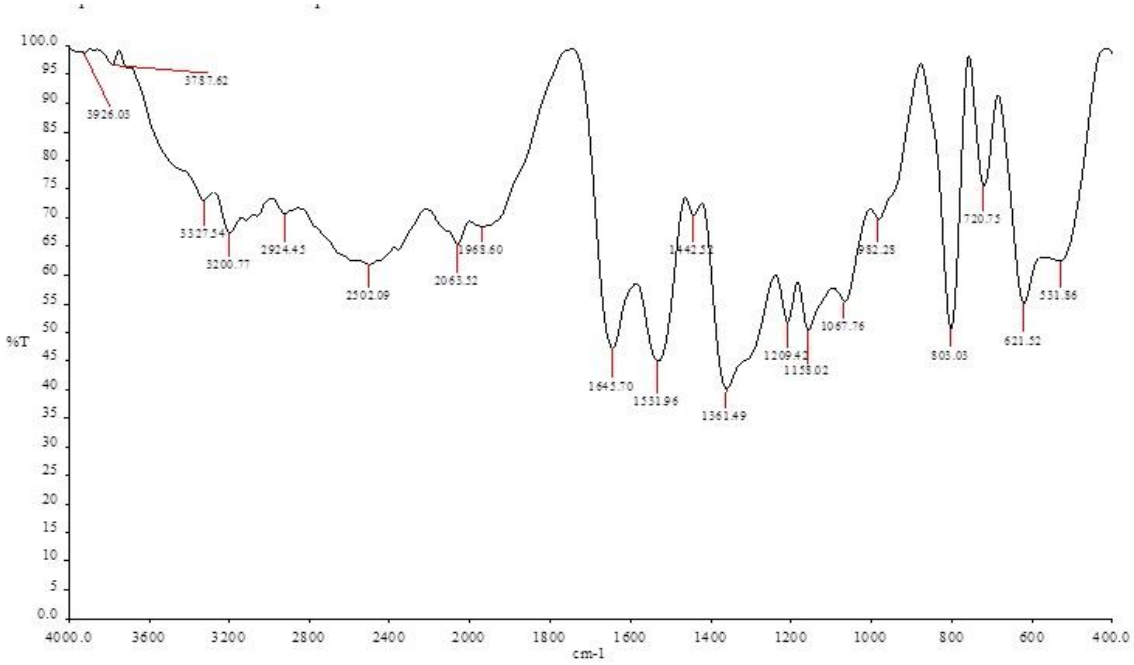

Fig. 7. The FTIR spectrum of the DMAPAB crystal

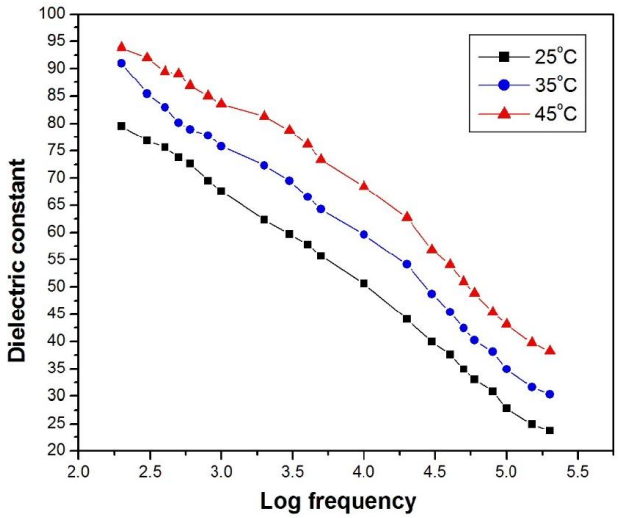

Fig. 8. The plot of dielectric constant (ε_r) and frequencies

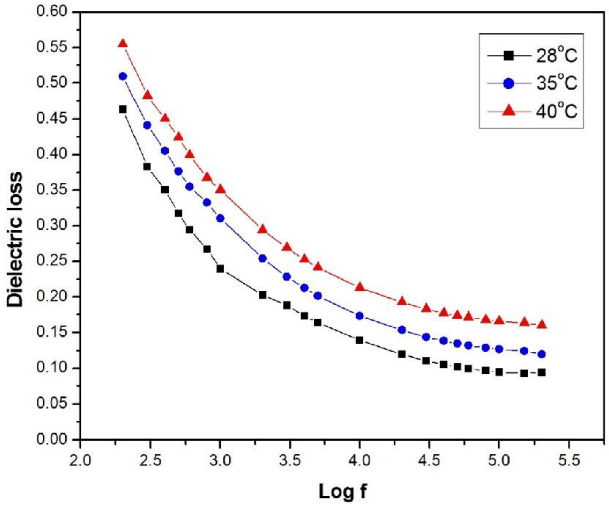

Fig. 9.The function of dielectric loss with log frequency

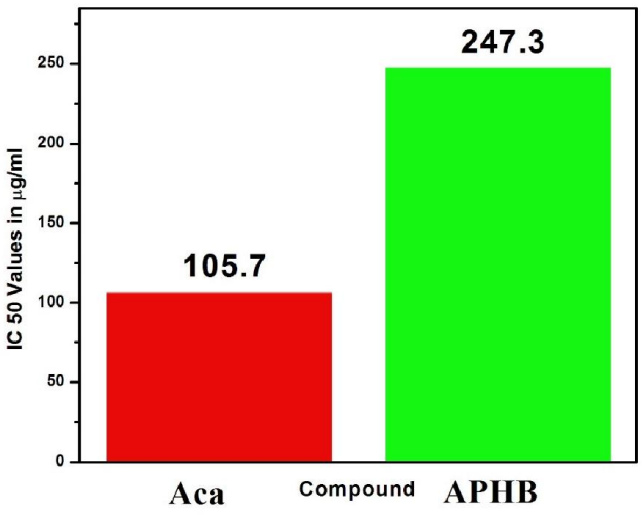

Fig. 10. The scavenging ability of DMAPAB crystal

The vibrations of various functional groups present in the crystal is analysed through absorption peaks. The NH stretching vibrational frequency in amine functional group is absorbed at 3327 cm^{-1}. The absorption bands at 3200 cm^{-1} and 2502 cm^{-1} are assigned to OH stretching vibration. The CH stretching mode vibration is obtained at 2924 cm^{-1}. In addition, the peaks at 2063 and 1968 cm^{-1} are attributed to CN stretching vibration. The OH bending vibrational mode is absorbed at 1645 cm^{-1}. The symmetric and asymmetric stretching modes of NO are revealed through the peaks at 1361 and 1531 cm^{-1} respectively. The peaks at 1209 cm^{-1} is assigned for the CO stretching mode. The peaks at 1158 and 621 cm^{-1} are attributed to CH in-plan and out-plan bending vibration. The CH wagging vibrational frequency is absorbed at 1067 cm^{-1}. The peak at 982 cm^{-1} is assigned for OH bending mode vibration. The NH wagging vibration is absorbed at 803 cm^{-1}. The peak at 720 cm^{-1} is assigned to the vibration of CH rocking mode.

Dielectric study

Dielectric measurement is one of the technique to analysis the electrical response of solids. The study of the dielectric properties of solids gives the information about the electric field distribution within the solid. The frequency dependence of these properties gives a great insight into the material's applications. The different polarization mechanisms in grown crystal is understood from the study of dielectric constant as a function of frequency and temperature. The capacitance of the crystal is measured for the frequency range of 50Hz-200 kHz at various temperatures of 25°C, 35°C and 45°C. The plot of dielectric constant (ε_r) and frequencies is shown in the figure 8. The dielectric constant of the crystal is calculated by using the relation $\varepsilon_r = C_{crys}d/\varepsilon_0 A$, where C_{crys} is the capacitance of the crystal, d is the thickness of the sample, ε_0 is the permittivity of free space and A is the area of the sample used. The dielectric constant has higher values in the lower frequency region and then it decreases with an increasing frequency. The contribution of space charge, orientation, electronic, and ionic polarizations reduces gradually at higher frequencies. This is the reason for the low value of dielectric constant at higher frequencies. The defects have no long enough time to rearrange in response to the applied voltage at higher frequency (Zukowski *et al*., 1989). Hence the capacitance of the sample decreases with increasing frequency. The function of dielectric loss with log frequency is shown in figure 9. The characteristic of low dielectric loss at high frequencies for a given sample suggested that the sample possesses an enhanced optical quality with lesser defects.

Thermodynamic properties

Several thermodynamic properties such as Zero Point Vibrational Energy (ZPVE), heat capacity (C_V), entropy (S) and rotational constants can be used to calculate the other thermodynamic energies and estimate the directions of chemical reactions according to relationships of thermodynamic functions and using second law of thermodynamics. On the basis of vibrational analysis, the Zero Point Vibrational Energy, heat capacity, entropy and rotational constants of the title compound have been calculated by the density functional method using 6-311++G basis set. The calculated thermodynamic properties are listed in Table 3. The DMAPAB molecules has ZPVE as 225.803 K Cal mol^{-1}, CV as 61.287 Cal $mol^{-1}K^{-1}$ and total thermal energy as 236.443 K Cal mol^{-1}. The thermodynamic data may provide useful information for the further study on the title compound.

Hyperpolarisability

The interactions of electromagnetic fields in various materials produce the nonlinear optical (NLO) effects by altering the phase, frequency, amplitude or other propagation characteristics from the incident fields (Sun *et al*., 2009). To design the novel NLO materials, the theoretical investigation plays a key role in understanding the structure–property relationship. As the basis becomes larger, one expects a better description of the compound and accordingly more accurate results. In the view of these points, B3LYP/6-311G++(d,p) method has been used for the present study. The complete equations for calculating the magnitude of the total static dipole moment (μ), mean polarizability (α), anisotropy of polarizability ($\Delta\alpha$) and first order hyperpolarizability (β) from Gaussian output are given below

$$\mu = \sqrt{\left(\mu_x{}^2 + \mu_x{}^2 + \mu_x{}^2\right)} \quad \ldots\ldots\ldots(16)$$

$$\alpha = \frac{(\alpha_{xx}+\alpha_{yy}+\alpha_{zz})}{3} \quad \ldots\ldots\ldots(17)$$

$$\Delta\alpha = \sqrt{2}\left[\left(\alpha_{xx} - \alpha_{yy}\right)^2 + \left(\alpha_{yy} - \alpha_{zz}\right)^2 + (\alpha_{zz} - \alpha_{xx})^2 + 6\alpha_{xx}^2\right]^{1/2} \quad \ldots\ldots\ldots(18)$$

$$\beta = \left[\left(\beta_{xxx} + \beta_{xyy} + \beta_{xzz}\right)^2 + \left(\beta_{yyy} + \beta_{yzz} + \beta_{yxx}\right)^2 + \left(\beta_{zzz} + \beta_{zxx} + \beta_{zyy}\right)^2\right]^{1/2} \quad \ldots\ldots\ldots(19)$$

The polarizabilities and hyperpolarizability are reported in terms of atomic units (a.u) and the calculated values have been converted by using 1 a.u. = 0.1482 x 10^{-24} esu for α and 1 a.u. = 8.6393 x 10^{-33} cm5/esu for β. In the calculations, the values of the calculated dipole moment (μ), mean polarizability (α) and anisotropy of polarizability ($\Delta\alpha$) are 11.3713Debye, 0.486Å esu, 0.937 Å esu. The calculated first hyperpolarizability value (β) which is an important key factors for NLO properties of molecular system is equal to 1.494 x 10^{-31} cm^5 esu^{-1}. In NLO studies, the urea is used as reference and its calculated values of μ, α, $\Delta\alpha$ and β are found to be 4.303 Debye, 0.139 Å esu, 0.934 Å esu, 0.563 x 10^{-31} cm^5 esu^{-1}respectively. In comparison with urea, the hyperpolarizability value of DMAPAB is more than two times that of urea.

Antibacterial activity

In vitro, the bacteria species Staphylococcus aureus, Bacillus substilis, Klebsiella pneumonia, and Pseudomonas aeruginosa were prepared in the disc with the concentration of 100µg/disc. Ciprofloxacin was used as a standard drug to compare the activity results. The screening data of the sample and standard

materials are given in Table 4. From the data, it is inferred that the cytotoxic activity is dose dependent. The synthesized compound shows good activity compare with standard drug. Among the number of bacterial species, the growth of Staphylococcus aureus was arrested to the larger amount than the other bacteria species. Nevertheless the synthesized compound molecule was active against the all bacterial species, it could reach the efficiency of standard drug to control the growth of bacteria. The result shows that the compound has potency for antibacterial activity.

Antifungal activity

The synthesized DMAPAB compound was also analysed for its antifungal activity using Clotrimazole as a standard drug for comparison of antifungal activity. The antifungal inhibition activity results of standard drug and synthesized compound are given in Table 5. The data confirms that the DMAPAB shows good inhibition activity against various fungal species. The DMAPAB compound also shows appreciable inhibition activity against *Candida albicans and Aspergillusfumigatus*. It is observed that the compound has the efficiency of antifungal activity.

Antioxidant activity

The DPPH method is simple, rapid and convenient method for scavenging of free radical. This method is widely used to examine the antioxidant properties of the compound. In the presence of compound, the stable DPPH radicals are capable of donating hydrogen atoms. Hence, the radical property is destroyed resulting in the colour change. The free radical scavenging ability of the synthesized compound with DPPH radical is studied in this analysis. The ascorbic acid was used as standard complex for comparison of results. The scavenging ability of the tested compound is represented in Figure 10. The result confirms that the synthesized compound can reduce the concentration of the initial free DPPH radicals. The IC 50 value of the BPHB compound is 263.7 µg/ml, whereas that for ascorbic acid is 119.6 µg/ml. This study confirms that the synthesized BPHB compound is capable of scavenging free radicals.

Conclusion

The hydrogen bonded charge transfer complex of N, N dimethyl 4-amino pyridinium 4-amino benzoate dihydrate was synthesized and grown successfully by slow evaporation technique at room temperature. The centrosymmetry space group and structure of the grown crystal were confirmed by the single crystal XRD analysis. A widespread hydrogen bonding network takes place due to the transfer of proton from acceptor moiety to the donor moiety. The presence of various functional groups in crystal was analyzed by The FTIR spectrum. UV-vis absorption analysis showed the appearance of the charge transfer band in UV– Visible spectrum of the title complex. This obviously confirms the formation the intermolecular CT crystal. The characteristic of low dielectric loss at high frequencies for grown crystals suggested that the grown crystals possessed enhanced optical quality with lesser defects. The Mulliken atomic charge and HOMO-LUMO energy for the compound were determined. Thermodynamic properties also have been calculated. Furthermore, the complex has been put in to observe their biological activity. Antimicrobial studies reveal that the complex showed a good inhibition activity against a panel of bacterial and fungal species. The antioxidant activity confirmed that the charge transfer complex can serve as possible antioxidant against DPPH radical.

REFERENCES

Al-Hashimi, Y.A. Hussein, Ab initio study on the formation of triiodide CT complex from the reaction of iodine with 2,3-diaminopyridine, 2010, Spectrochim. Acta, Part A 75 (1): 198 -202.

Amin A.S., G.O. El-Sayed, Y.M. Issa,Utility of certain π-acceptors for the spectrophotometric determination of norfloxacin, 1995, Analyst 120 (4): 1189 - 1193.

Bauer A.W., W.M.M. Kirby, J.C. Sherries, M. Truck, Antibiotic susceptibility testingby a standardized single disk method, 1996, *Am. J. Cl in. Pathol*., 45 : 493 - 6.

Becke A.D., Densityfunctional thermochemistry. III. The role of exact exchange, 1993, *J. Chem. Phys*., 98, 5648 - 52

Blois, M.S., Antioxidant determinations by the use of a stable free radical, 1958, *Nature*, 29:1199-1200.

Bock H., N. Nagel, A. Seibel, Interactions in Molecular Crystals, 123. Crystallization and Structure of Donor–Acceptor Complexes between Rigid or Conformationally Flexible Thio-Crowns and Iodine, 1997, *Euro. J. Org. Chem*., 10: 2151 - 2159.

Chermette H., Chemical reactivity indexes in density functional theory, 1999, *J. Comput. Chem.,* 20: 129–154.

Collins A.H. (Ed.), Microbiology Method, second ed., Butterworth, London, 1976.

Cruickshank R., J.P. Duguid, B.P. Marmion, R.H.A. Awain, Medicinal Microbiology, 12th ed., Vol II, Churchill Livingstone, London, 1995, p. 196 - 202.

Enraf-Nonius, CAD-4 EXPRESS Version 5.1/1.2., 1994, Enraf-Nonius, Delft, The Netherlands.

Farrugia L.J., ORTEP-3 for Windows - a version of ORTEP-III with a Graphical User Interface (GUI), 1997, J. *Appl. Crystallogr*., 30 : 565.

Frischv, G.W. Trucks, H.B. Schlegel, G.E. Scuseria, M.A. Robb, J.R. Cheeseman, J.A. Montgomery, Jr., T. Vreven, K.N. Kudin, J.C. Burant, J.M. Millam, S.S. Iyengar, J. Tomasi, V. Barone, B. Mennucci, M. Cossi, G. Scalmani, N. Rega, G.A. Petersson, H. Nakatsuji, M. Hada, M. Ehara, K. Toyota, R. Fukuda, J. Hasegawa, M. Ishida, T. Nakajima, Y. Honda, O. Kitao, H. Nakai, M. Klene, X. Li, J.E. Knox, H.P. Hratchian, J.B. Cross, V. Bakken, C. Adamo, J. Jaramillo, R. Gomperts, R.E. Stratmann, O. Yazyev, A.J. Austin, R. Cammi, C. Pomelli, J.W. Ochterski, P.Y. Ayala, K. Morokuma, G.A. Voth, P. Salvador, J.J. Dannenberg, V.G. Zakrzewski, S. Dapprich, A.D. Daniels, M.C. Strain, O. Farkas, D.K. Malick, A.D. Rabuck, K. Raghavachari, J.B. Foresman, J.V. Ortiz, Q. Cui, A.G. Baboul, S. Clifford, J. Cioslowski, B.B. Stefanov, G. Liu, A. Liashenko, P. Piskorz, I. Komaromi, R.L.Martin, D.J. Fox, T. Keith, M.A. Al-Laham, C.Y. Peng, A. Nanayakkara, M. Challacombe, P.M.W. Gill, B. Johnson, W. Chen, M.W. Wong, C. Gonzalez, J.A. Pople, Gaussian 03, Revision C.02, Gaussian Inc., Wallingford CT, 2004.

Goel A., V.J. Ram, Natural and synthetic 2H-pyran-2-ones and their versatility in organic synthesis, 2009, Tetrahydron 65: 7865 - 7913.

Gutmann F., C. Johnson, H. Keyzer, J. Molnar, Charge Transfer Complexes in Biochemistry System, Marcel Dekker Inc., 1997.

Koopmans T.A., Ordering of Wave Functions and Eigenenergies to the Individual Electrons of an Atom, 1993, *Physica*1: 104 - 113

Kosar B. and C. Albayrak, pectroscopic investigations and quantum chemical computational study of (E)-4-methoxy-2-[(*p*-tolylimino) methyl] phenol, 2011, *Spectrochim. Acta* A, 78: 160 - 167.

Lee C., W.T. Yang, R.G. Parr, Development of the Colle-Salvetti correlation-energy formula into a functional of the electron density, 1988, Phys. Revi. B 37: 785 - 789.

Macrae C.F., I.J. Bruno, J.A. Chisholm, P.R. Edgington, P. McCabe, E. Pidcock,L. Rodriguez-Monge, R. Taylor, J. van de Streek, P.A. Wood, Mercury CSD 2.0 - New Features for the Visualization and Investigation of Crystal Structures, 2008, *J. Appl. Crystallogr*., 41 : 466 - 470.

Misoguti L., A.T. Varela, F.D. Nunes, V.S. Bagnato, E.E.A. Melo, J.M. Filho, S.C. Zilio,Optical properties of L-alanine organic crystals, 1996, Opt. Mater. 6 : 147 - 152.

North A.C.T., D.C. Phillips, & F.S. Mathews, A Semi-Empirical Method of Absorption Correction, 1968, *ActaCryst. Sect*. A 24 (3): 351-353.

Ogorodnikov I.N., V.A. Pustovarov, A.A. Goloshumova, L.I. Isaenko, A.P. Yelisseyev, V.M. Pashkov, A luminescence spectroscopy study of SrI2:Nd3+ single crystals, 2013, *J. Lumin*., 143 : 101 -107.

Parr R.G., L.V. Szentpaly and S. Liu, Electrophilicity Index, 1999, *J. Am. Chem. Soc.,*121 (9): 1922 - 1924.

Parthasarathi R., V. Subramanian, D.R. Roy, P.K. Chattaraj, Electrophilicity index as a possible descriptor of biological activity, 2004, *Bioorg. Med. Chem*., 12 : 5533–5543.

Sheldrick G. M., SHELXL97and SHELXS97, Program for crystal structure solution. 1997: University of Gottingen, Germany.

Sun Y.X., Q.L. Hao, W.X. Wei, Z.X. Yu, L.D. Lu, X.Wang, Y.S. Wang, Experimental and density functional studies on 4-(3,4-dihydroxybenzylideneamino)antipyrine, and 4-(2,3,4-trihydroxybenzylideneamino)antipyrine, 2009, *J. Mol. Struct.: Theochem.,* 904 : 74-82.

Yasutake M., K. Araki, M. Zhou, R. Nogita, T. Shinmyozu, Solid-State Structural Study of the Charge-Transfer Complexes of 5,7,9-Trimethyl- and 2,11,20-Trithia[33](1,3,5)cyclophanes, 2003, Eur. J. Organic Chem. 7: 1343 - 1351.

PalaciosR.E., G. Kodis, S.L. Gould, de la L. Garza, A. Brune, D. Gust, T.A. Moore, Artificial Photosynthetic Reaction Centers: Mimicking Sequential Electron and Triplet-Energy Transfer, 2005, Chem. Phys. Chem. 6 : 2359 - 2370.

Zhao F.L., B.Z. Xu, Z.Q. Zhang, S.Y. Tong, Study on the charge-transfer reaction between 7,7,8,8-tetracyanoquinodimethane and drugs, 1999, J. Pharm. Biomed. Anal. 21 : 355 - 360.

Zukowski, P.W. Kantorow, S.B. Aczka, D. Stelmakh, V.F., Processes of Radiation Defect Interaction and Amorphisation of Silicon at Large Implantation Doses, 1989, *Phys. Stat. Sol.* A112: 695 - 698.

****